

An error-minimizing approach to inverse Langevin approximations

Benjamin C. Marchi¹ · Ellen M. Arruda^{1,2,3}

Received: 11 June 2015 / Revised: 7 August 2015 / Accepted: 17 September 2015 / Published online: 16 October 2015
© Springer-Verlag Berlin Heidelberg 2015

Abstract The inverse Langevin function is an integral component to network models of rubber elasticity with networks assembled using non-Gaussian descriptions of chain statistics. The non-invertibility of the inverse Langevin often requires the implementation of approximations. A variety of approximant forms have been proposed, including series, rational, and trigonometric divided domain functions. In this work, we develop an error-minimizing framework for determining inverse Langevin approximants. This method can be generalized to approximants of arbitrary form, and the approximants produced through the proposed framework represent the error-minimized forms of the particular base function. We applied the error-minimizing approach to Padé approximants, reducing the average and maximum relative errors admitted by the forms of the approximants. The error-minimization technique was extended to improve standard Padé approximants by way of understanding the error admitted by the specific approximant and using error-correcting functions to minimize the residual relative error. Tailored approximants can also be constructed by appreciating the evaluation domain of the application implementing the inverse Langevin function. Using a non-Gaussian, eight-chain network model of rubber elasticity, we show

how specifying locations of zero error and reducing the minimization domain can shrink the associated error of the approximant and eliminate numerical discontinuities in stress calculations at small deformations.

Keywords Inverse Langevin function · Rubber elasticity · Statistical mechanics · Non-Gaussian chain statistics · Padé approximation

Introduction

Approximations are fundamental to solving real problems in science and engineering. Often, the sheer complexity of systems necessitates simplification, but there are also situations where no closed form solution exists. This is where numerical approximations enter. Numerical techniques and solutions are ubiquitous in problems of applied solid and fluid mechanics, heat transfer, and control theory. While approximations are convenient, and sometimes necessary, not fully appreciating how approximations affect the solution can diminish their power. Network-based models of rubber elasticity built from non-Gaussian statistical representations of long chain molecules typically require determining the inverse Langevin of an argument. The Langevin function is defined as follows

$$\mathcal{L}(x) = \coth(x) - \frac{1}{x}. \quad (1)$$

While computing the Langevin is straightforward, there exists no closed form expression for the inverse Langevin function, $\mathcal{L}^{-1}(x)$. Since network models typically require an explicit definition for the inverse Langevin function, they naturally employ approximations. Nevertheless, network models have had great success in describing the large

✉ Benjamin C. Marchi
bmarchi@umich.edu

¹ Department of Mechanical Engineering, University of Michigan, Ann Arbor, MI, USA

² Department of Biomedical Engineering, University of Michigan, Ann Arbor, MI, USA

³ Department of Macromolecular Science and Engineering, University of Michigan, Ann Arbor, MI, USA

strain and finitely extensible behavior of elastomeric materials (Arruda and Boyce 1993; Boyce and Arruda 2000; Flory and Erman 1982; Treloar 1975; Wang and Guth 1952; Wu and Van der Giessen 1993), and recently, biological cellular and tissue structures (Bischoff et al. 2002a, b; Kang et al. 2008; Kuhl et al. 2005; Ma and Arruda 2013; Ma et al. 2010; Palmer and Boyce 2008). While network models of nonlinear elasticity constructed with non-Gaussian statistics have been impressive, their efficacy can be limited by non-optimal inverse Langevin function approximations.

Macromolecular elastomers are principally composed from randomly oriented, loosely cross-linked, long-chain molecules with weak or sparse intra-molecular interactions. A molecular chain contained in a representative volume element of a network-based model can be modeled as N freely rotating rigid Kuhn segments each of length l (Kuhn and Gr \ddot{u} n 1942). A Freely Jointed Chain (FJC) has an end-to-end distance vector of magnitude r . Assuming each chain link is completely random and independent from all other links in the chain, the probability density, $p(r)$, of link angles, with respect to r , is given by

$$\ln(p(r)) = c - N \left(\frac{r}{Nl} \beta + \ln \left(\frac{\beta}{\sinh(\beta)} \right) \right) \quad (2)$$

where c is a constant and β is defined as

$$\beta = \mathcal{L}^{-1} \left(\frac{r}{Nl} \right). \quad (3)$$

It is important to note that at this point in the development of non-Gaussian single chain behavior an approximation is already being made. The probability density is derived using the Stirling's approximation to simplify expressions involving factorials; therefore, any constitutive model built with non-Gaussian FJCs with link angle probability density functions including the inverse Langevin has already introduced error into the analysis (Kuhn and Gr \ddot{u} n 1942; Treloar 1975).

The force-extension relationship for a single FJC is determined by differentiating the entropy function, $s = k \ln(p(r))$, yielding

$$f = -T \frac{\partial s}{\partial r} = \frac{kT}{l} \mathcal{L}^{-1} \left(\frac{r}{Nl} \right) \quad (4)$$

where k is the Boltzmann constant and T is the absolute temperature.

Three-dimensional networks of finitely extensible, non-Gaussian chains with this force-extension relationship can be arranged in a variety of configurations and aspect ratios to describe macroscopic stress-strain behavior (Arruda and Boyce 1993; Bischoff et al. 2002a, b; Boyce and Arruda 2000; Flory and Erman 1982; Kang et al. 2008; Kuhl et al. 2005; Ma and Arruda 2013; Ma et al. 2010; Palmer and Boyce 2008; Treloar 1975; Wang and Guth 1952; Wu and Van der Giessen 1993). These network constitutive

models are dependent on the inverse Langevin function. Numerically solving the inverse Langevin function can be accomplished through a nonlinear root-finding problem. This iterative problem is computationally costly to solve, and as the scale of the problem increases, especially in the context of finite element analyses, the complexity of the constitutive law begins to dominate total solution time. Approximants reduce the computational burden of computing the inverse Langevin function by substituting a straightforward function evaluation for the iterative root-finding problem.

In this work, we examine approximate solutions to the inverse Langevin function through an error-based approach in an effort to construct approximants that are decidedly accurate without sacrificing computational fidelity. This is accomplished by understanding how the general form of a particular approximation behaves relative to the exact inverse Langevin function and minimizing the relative error of the approximant over its entire domain. This approach yields an error-minimized approximant of a particular form. Additionally, regardless of the form of the approximant, due to the non-invertibility of the Langevin function, residual error will exist. This error can be minimized, increasing the quality of the approximant, through correcting functions that modify the behavior of the original approximation.

Examining the quality of a candidate approximant through error-based techniques can also provide insight into how the approximant affects constitutive stress-strain behavior, potentially avoiding costly inconsistencies during large strain analyses of complex deformations. The form of the approximant may be modified such that it eliminates small stretch stress discontinuities by construction. This can be accomplished by stipulating zero approximant error at particular locations in the domain $x \in [0, 1]$ or by understanding the evaluation domain necessary for a precise application implementing the inverse Langevin function and reducing the valid optimization domain within the proposed error-minimization framework.

Inverse Langevin approximations

There has been considerable work, including many recent efforts (Darabi and Itskov 2015; Itskov et al. 2009, 2012; Jedynak 2015), in the development of simple and accurate functions that behave similarly to the inverse Langevin function (Cohen 1991; Kuhn and Gr \ddot{u} n 1942; Puso 1994; Treloar 1975; Warner Jr 1972). Many of these approximations are constructed from Taylor series expansions or Pad \acute{e} approximants; however, many forms exist (Bergstr \ddot{o} m 1999).

Taylor series approximants

Though no closed form of the inverse Langevin exists, it is possible to construct high-order, finite series expansions to approximate the behavior of the function. The Taylor series is a powerful tool that can be used to determine a series description of a function, and it is possible, through the use of the Lagrange inversion formula, to find the Taylor expansion of the inverse of a function. The use of a Taylor series about the point $x = 0$ to approximate the inverse Langevin function, $\mathcal{L}^{-1}(x)$, was first proposed by Kuhn and Grün (1942). Using the first four nonzero terms of the Taylor expansion, Kuhn and Grün proposed the following approximation

$$\mathcal{L}^{-1}(x) = 3x + \frac{9}{5}x^3 + \frac{297}{175}x^5 + \frac{1539}{875}x^7 + O(x^9). \tag{5}$$

$$\begin{aligned} \mathcal{L}^{-1}(x) = 3x + \frac{9}{5}x^3 + \frac{297}{175}x^5 + \frac{1539}{875}x^7 + \frac{126117}{67375}x^9 + \dots \\ + \frac{519588001407316958447129785511020819131555326399179970047767492196701159}{902903623205422824379381653441368510859764577156376354396343231201171875}x^{59} + O(x^{61}). \end{aligned} \tag{7}$$

High-order Taylor series representations of the inverse Langevin have the advantage of excellent agreement with the exact inverse Langevin function around the point of expansion; however, in the neighborhood of the singular point at $x = 1$, Taylor expansions diverge significantly. This is a fundamental limitation of the form of the series. Despite this drawback, the 115 term series expansion has superior accuracy compared to a selection of rational approximations (Cohen 1991; Puso 1994; Treloar 1975) in the region $x \in [0, 0.95]$ (Itskov et al. 2012)

Padé approximants

To combat the inability of Taylor series expansions to accurately describe the behavior of the inverse Langevin function near the singular point $x = 1$, rational functions have been proposed as approximants. Fractions of polynomials have the advantage of admitting asymptotic behavior within a finite domain. Padé approximants—typically a particular Padé approximation is denoted as an $[m/n]$ approximant, where m and n are the orders of the numerator and denominator polynomials, respectively—have had great success in accurately describing the inverse Langevin function $\forall x \in [0, 1]$, while simultaneously capturing the asymptotic character at the singular point. Two methods have been used to construct Padé approximations of the inverse Langevin function: single-point and multipoint Padé approximations.

The series was expanded in Itskov et al. (2009) to include the first 20 nonzero terms yielding

$$\begin{aligned} \mathcal{L}^{-1}(x) = 3x + \frac{9}{5}x^3 + \frac{297}{175}x^5 + \frac{1539}{875}x^7 + \frac{126117}{67375}x^9 \\ + \frac{43733439}{21896875}x^{11} + \frac{231321177}{109484375}x^{13} \\ + \frac{20495009043}{9306171875}x^{15} + \frac{1073585186448381}{476522530859375}x^{17} \\ + \frac{4387445039583}{1944989921875}x^{19} + O(x^{21}). \end{aligned} \tag{6}$$

Itskov et al. (2012), with computational efficiencies provided by Dargazany et al. (2013), developed a rapid and numerically simple recursive algorithm for determining the Taylor coefficients of the inverse of a series. Using the inverse Langevin as a model, Itskov et al. (2012) extended the Taylor series expansion of the inverse Langevin as

A single-point Padé approximation is built from information of the function and its derivatives at the point of expansion. This information is readily available in an exact form from the Taylor series expansion of the inverse Langevin. The single-point approach has been an incredibly popular technique for constructing inverse Langevin approximants, including the rounded Treloar [1/6] approximation (1975)

$$\mathcal{L}^{-1}(x) = \frac{3x}{1 - 0.6x^2 - 0.2x^4 - 0.2x^6}, \tag{8}$$

the rounded Warner [1/2] approximation (1972)

$$\mathcal{L}^{-1}(x) = \frac{3x}{1 - x^2}, \tag{9}$$

the Cohen [3/2] approximation (1991)

$$\mathcal{L}^{-1}(x) = x \frac{3 - 36/35 x^2}{1 - 33/35 x^2}, \tag{10}$$

the rounded Cohen [3/2] approximation (1991)

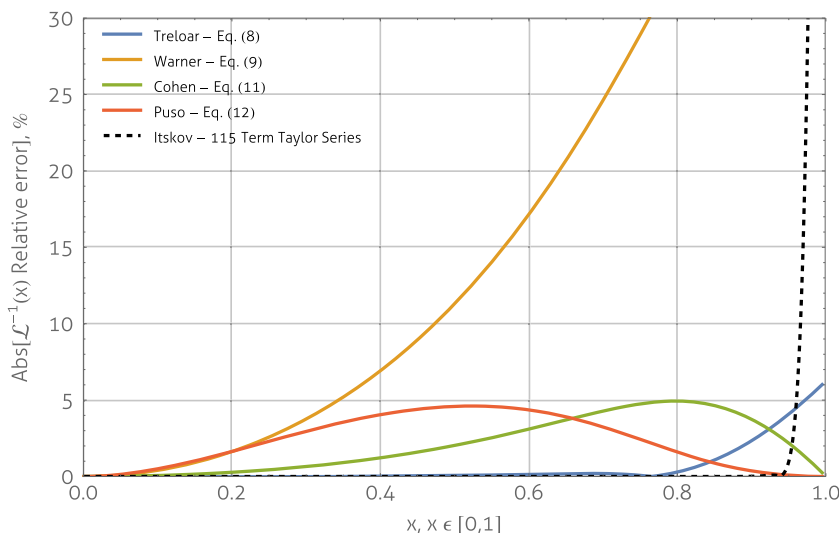
$$\mathcal{L}^{-1}(x) = x \frac{3 - x^2}{1 - x^2}, \tag{11}$$

and the rounded Puso [1/3] approximation (2003)

$$\mathcal{L}^{-1}(x) = \frac{3x}{1 - x^3}. \tag{12}$$

The extent of coefficient rounding and the form of the proposed function differentiate these approximations. Each

Fig. 1 Percent relative error of Taylor series expansion and single-point Padé approximations of the inverse Langevin function



approximation can be evaluated by determining its error relative to the exact inverse Langevin function. Figure 1 compares the percent relative error of each of the single-point Padé approximants, as well as the 115-term Taylor series expansion proposed by Itskov et al. (2012). It is clear how the form of the approximation can have a profound impact on the evolution of error within the domain $x \in [0, 1]$; particularly, the approximations from Cohen (1991) and Puso (1994) are able to capture the asymptotic behavior of the inverse Langevin at the singular point.

In multipoint Padé approximations, sometimes called rational interpolants or Newton-Padé approximants, the coefficients of the approximant are found using information about the function at a series of points within its domain (see Holub (2003) for a complete discussion of the technique). By evaluating the Padé approximant at each of the interpolation points, it is possible to construct a linear system to determine the coefficient values—for uniqueness of the approximant, typically, a normalizing condition is also imposed. The accuracies of approximants produced by this method are highly dependent on the selection of interpolation points. Recently, multipoint Padé approximants have been shown to have increased accuracy compared to traditional single-point Padé approximants (Darabi and Itskov 2015; Jedynak 2015). As with single-point Padé approximants, multipoint approximants can be differentiated by the orders of polynomials used in their construction. The following approximants have been proposed for the inverse Langevin function: the rounded Jedynak [3/2] approximation (2015)

$$\mathcal{L}^{-1}(x) = x \frac{3.0 - 2.6x + 0.7x}{(1-x)(1+0.1x)}, \tag{13}$$

and the rounded Darabi [3/1] approximation (2015)

$$\mathcal{L}^{-1}(x) = x \frac{x^2 - 3x + x}{1 - x}. \tag{14}$$

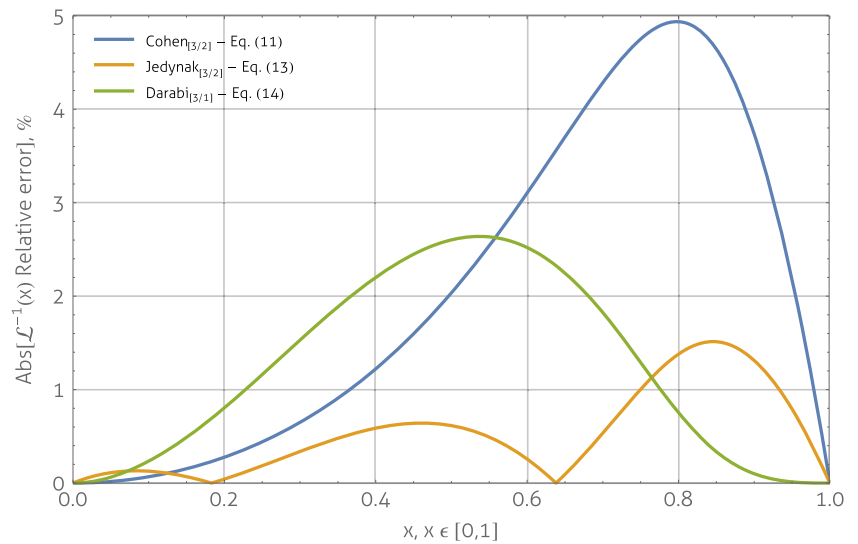
Figure 2 illustrates the ability of multipoint approximants to reduce error compared to single-point approximants of a similar form. Approximants proposed by Jedynak (2015) and by Darabi and Itskov (2015) admit a maximum relative error of 1.514 and 2.639 %, respectively, compared to the 4.937 % maximum relative error of the rounded Cohen approximation (1991).

Recently, a mathematical scheme for determining approximants has been proposed by Kröger (2015) that accounts for the exact asymptotics, symmetry, and integral behavior of the inverse Langevin by construction. While approximants established by satisfying the requirements detailed in Kröger (2015) are strictly admissible in the context of function behavior, the approximants tend to admit a larger maximum relative error compared to approximants of similar constituent polynomial order. This error increase can be attributed, in part, to the symmetry requirement, which can be easily accounted for by using the domain $x \in [0, 1]$ in the construction of the approximant and numerically satisfying the symmetry in the implementation of the approximant by letting $\mathcal{L}^{-1}(x) = \text{sign}(x) \mathcal{L}^{-1}(|x|)$, taking advantage of the odd behavior of the inverse Langevin function.

Divided domain approximants

Non-Taylor and Padé approximants also exist for the inverse Langevin function. Primarily, Bergström (1999) proposed a piecewise defined approximant, with its domain divided

Fig. 2 Percent relative error of multipoint Padé approximates compared to the rounded Cohen [3/2] approximation



to more accurately describe the asymptotic behavior of the inverse Langevin function. Bergström (1999) proposed a dual interval approximant defined by

$$\mathcal{L}^{-1}(x) = \begin{cases} 1.31446 \tan(1.58986x) + 0.91209x, & |x| < 0.84136 \\ 1/(\text{sign}(x) - x), & 0.84136 \leq |x| < 1. \end{cases} \quad (15)$$

The Bergström approximation and, more generally, approximations of its type have a number of restrictions. The main challenge in the implementation of the Bergström approximant is the discontinuity as the function transitions between its domains. Numerically, this discontinuity can be problematic in the calculation of deformation distributions, or in systems that require integration or differentiation of the inverse Langevin function, such as in calculating the chain free energy of rubber-like materials. Despite the limitations of the Bergström approximation, the approximant is highly accurate in describing the inverse Langevin function. In the domain $x \in [0, 1]$, the approximant has a maximum relative error of $6.325 \times 10^{-2} \%$.

Error-corrected approximations

Understanding the behavior of the error admitted by a particular approximant is as important as the form of the original approximation. Every approximant of the inverse Langevin function will result in residual error. By examining the form of the error function, it is possible to supplement the original approximation with an error correcting function to minimize the error produced by the approximation.

Nguessong et al. (2014), using the Cohen approximation as the base approximant for the inverse Langevin function

and a two-stage correction procedure proposed by Beda and Chevalier (2003), showed the ability of a simply correcting function to dramatically reduce the residual error of the Cohen approximation. The Cohen approximation can be written to include its error term as

$$\mathcal{L}^{-1}(x) = x \frac{3 - x^2}{1 - x^2} + O(x) \quad (16)$$

where $O(x)$ is the absolute error of the Cohen approximation. Graphically, it can be seen that $O(x)$ takes the form

$$O(x) \approx Ax^\alpha. \quad (17)$$

It is possible to determine the parameters A and α that minimize the absolute error of the Cohen approximation through a variety of curve fitting techniques. Nguesong et al. (2014) again examined the error committed by the approximation following the first-stage correction. The approximant, following the first correction, has the form

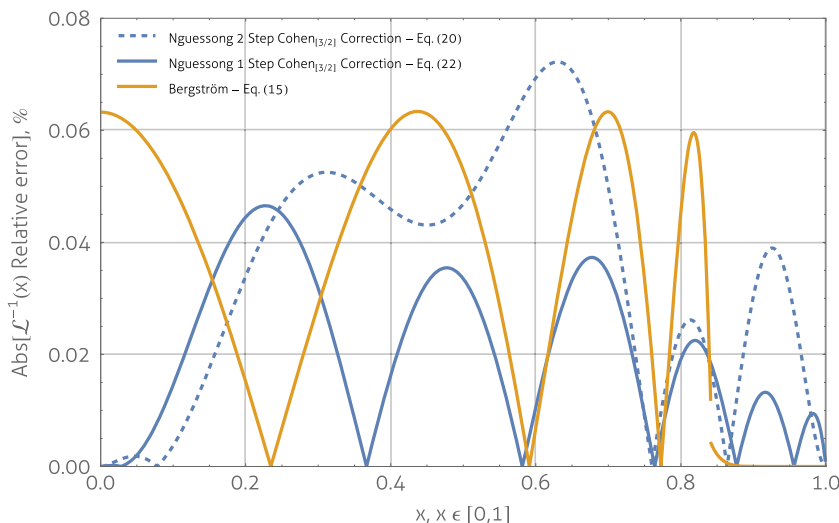
$$\mathcal{L}^{-1}(x) = x \frac{3 - x^2}{1 - x^2} + Ax^\alpha + O_2(x) \quad (18)$$

where $O_2(x)$ is the absolute error of the Cohen approximation, including the correcting effect of the first-stage improvement. The error function $O_2(x)$ behaves like a modulated polynomial with two roots, one located in the domain $x \in [0, 1]$ and the other at the singular point. Nguesong et al. (2014) proposed a second correcting function of the form

$$O_2(x) \approx Bx^\beta(x - \gamma)(x - \delta). \quad (19)$$

Requiring the zeros (γ and δ) of the correcting polynomial to be coincident with the roots of the error function $O_2(x)$, the parameters B and β can be readily determined by minimizing the difference between the proposed correction and error functions. This combined procedure yields a two-

Fig. 3 Percent relative error of error-corrected Cohen approximations and the Bergström approximant with respect to the inverse Langevin function



step error-corrected approximation built from the Cohen approximation (see Nguessong et al. (2014) for a detailed discussion of the method) expressed by

$$\mathcal{L}^{-1}(x) = x \frac{3 - x^2}{1 - x^2} - \frac{1}{2}x^{10/3} + 3x^5(x - 0.76)(x - 1) . \tag{20}$$

Once the form of the error-correcting functions have been determined, it is possible to write a generalized form for the Nguessong-type correction by combining the functions presented in Eqs. 17 and 19. The Nguessong-type correction approximation has the general form

$$\mathcal{L}^{-1}(x) = x \frac{3 - x^2}{1 - x^2} + Ax^\alpha + Bx^\beta(x - \gamma)(x - \delta) . \tag{21}$$

An improved correction function, as compared to the two-step correction, can be determined by minimizing the error committed by the general Nguessong-type correction approximation. Nguessong et al. (2014) found, while holding the parameters γ and δ fixed in Eq. 21 from the two-step procedure at 0.76 and 1, respectively, a least squares minimization yielding the following approximation

$$\mathcal{L}^{-1}(x) = x \frac{3 - x^2}{1 - x^2} - 0.488x^{3.243} + 3.311x^{4.789}(x - 0.76)(x - 1) . \tag{22}$$

Correcting functions can have a pronounced effect on the maximum relative error admitted by a particular approximation. The two approximations (20) and (22) reduce the relative error of the Cohen approximation from 4.937 % to 7.222×10^{-2} and 4.654×10^{-2} %, respectively. Figure 3 depicts the relative error admitted by the augmented Cohen approximations, with the Bergström approximant, Eq. 15, included for reference (note the discontinuity in Bergström approximant as the function transitions between domains).

Approximations with corrections built from standard functions produce new expressions that are straightforwardly evaluated, integrated, and differentiated while dramatically reducing the relative error of the original approximation.

An error-minimizing and error-correcting framework for determining inverse Langevin approximants

Minimized rational approximants

There has been substantial work in developing methods to construct accurate and computationally efficient approximations of the inverse Langevin function. These approximants, built from Taylor series expansions, Padé approximations, and divided domain composite functions, have been successful and generally accepted by the community. While accurate and largely robust, the real strength of these approximations is not necessarily their complete description of the approximant but in their identification of possible candidate forms for approximating the inverse Langevin function.

Moreover, multipoint Padé approximations are highly dependent on the interpolation points. Darabi and Itskov (2015) and Jedynak (2015) showed that small changes in the interpolation array can lead to spurious approximants, even resulting in non-characteristic artifacts like poles and zeros in the function domain $x \in [0, 1]$.

An alternative approach described herein is to build approximants from an error-minimization perspective. By fixing certain behavior of the potential approximant, like requiring the form of the approximant to automatically satisfy the asymptotic behavior at $x = 1$ and be well behaved at $x = 0$, the model function can be tuned to best represent

the features of the inverse Langevin function. Explicitly, let the approximant have the following characteristics

$$\mathcal{L}^{-1}(0) = 0, \tag{23}$$

$$\left. \frac{\partial \mathcal{L}^{-1}(x)}{\partial x} \right|_{x=0} = 3, \tag{24}$$

and

$$\lim_{x \rightarrow 1^-} \mathcal{L}^{-1}(x) \rightarrow \infty. \tag{25}$$

Accounting for the conditions described by Eq. 23 through (25), and avoiding complications manifesting from non-uniqueness, the general forms of the [3/1] and [3/2] Padé approximants presented by Dargazany et al. (2013) and Jedynek (2015), respectively, can be written as

$$\mathcal{L}_{[3/1]}^{-1}(x, \mathbf{a}) = x \frac{-3 + a_0x + a_1x^2}{x - 1}, \tag{26}$$

and

$$\mathcal{L}_{[3/2]}^{-1}(x, \mathbf{b}) = x \frac{3 + b_0x + b_1x^2}{(x - 1)(b_2x - 1)} \tag{27}$$

where a_i and b_i are constants left arbitrary.

The constant vectors $\mathbf{a} = \{a_0, a_1\}$ and $\mathbf{b} = \{b_0, b_1, b_2\}$ can be found by minimizing the relative error of the approximants presented in Eqs. 26 and 27 with respect to the

exact inverse Langevin function. Formally, the minimization objectives are

$$\underset{\mathbf{a}}{\text{minimize}} \left\{ \max_{x \in [0,1]} \left| \frac{\mathcal{L}_{[3/1]}^{-1}(x, \mathbf{a})}{\mathcal{L}^{-1}(x)} - 1 \right| \right\} \tag{28}$$

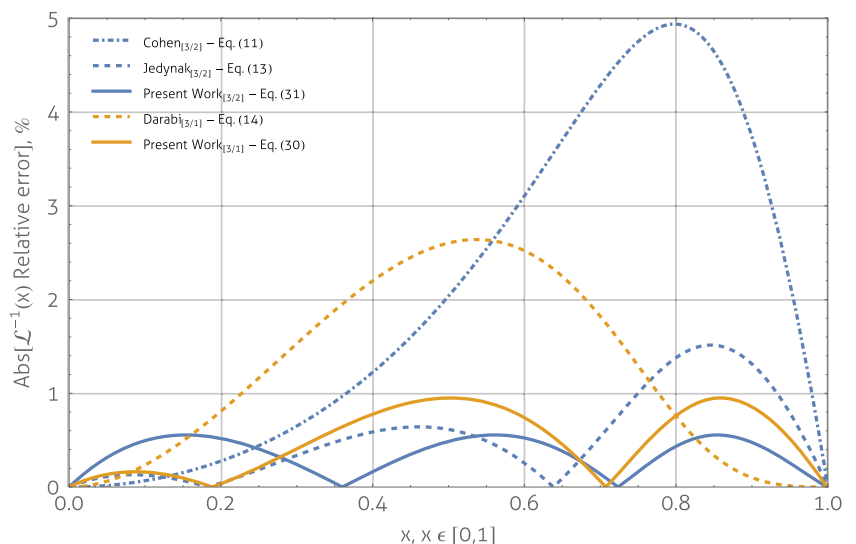
and

$$\underset{\mathbf{b}}{\text{minimize}} \left\{ \max_{x \in [0,1]} \left| \frac{\mathcal{L}_{[3/2]}^{-1}(x, \mathbf{b})}{\mathcal{L}^{-1}(x)} - 1 \right| \right\}. \tag{29}$$

There are a variety of numerical optimization algorithms that can be used to solve problems of this type. Nonlinear optimization can essentially be divided into gradient-based and direct search methods. Gradient methods use first and/or second derivative information to search the optimization space for optima. Sequential quadratic programming (SQP) is an example of a gradient-based method (Boggs and Tolle 1995). Direct search methods do not directly use gradient information. Differential evolution is an iterative, stochastic direct search optimization algorithm that can be applied to non-differentiable, non-continuous functions (Storn and Price 1997). Differential evolution maintains a population of trial solutions that are mated and evaluated at each iteration, traversing the solution space to find optima. The algorithm has incredible mobility with respect to solution spaces scattered with local optima (Storn and Price 1997).

Applying differential evolution, numerically implemented in Mathematica (Wolfram Research, Inc., Mathe-

Fig. 4 Comparison of [3/1] and [3/2] Padé and error-minimized approximations of the inverse Langevin function



matica, Version 10.0, Champaign, IL (2014)), to (28) and (29) yields the following approximations

$$\mathcal{L}_{[3/1]}^{-1}(x) = x \frac{-3 + 2.8811x - 0.8810x^2}{x - 1}, \tag{30}$$

and

$$\mathcal{L}_{[3/2]}^{-1}(x) = x \frac{3 + x(1.1564x - 3.3522)}{(0.1958x - 1)(x - 1)}. \tag{31}$$

The approximants presented in Eqs. 30 and 31 represent the particular relative error-minimized forms for the [3/1] and [3/2] Padé approximations, respectively. Allowing the coefficient vectors to remain arbitrary in the optimization, the proposed minimization framework reduces the maximum relative error of the [3/1] Padé approximant from 2.639 to 0.9500 % and the error of the [3/2] Padé approximant from 1.514 to 0.5554 %. The relative error of the approximants Eqs. 30 and 31 are compared to the Cohen (Eq. 11), Darabi (Eq. 14), and Jedynek (Eq. 13) approximations in Fig. 4.

From Fig. 4 it can be seen that the error-minimization procedure defined in the current work distributes the relative error admitted by a particular approximant over the entire domain $x \in [0, 1]$, producing a more consistently accurate approximation of the inverse Langevin function compared to approximants derived from single or multipoint Padé approximants. This feature of the approximant can be quantified by determining the average error. The average error of an approximant may be defined as

$$\text{error}_{\text{avg}} = \int_0^1 \left| \frac{\mathcal{L}_{\text{approx}}^{-1}(x)}{\mathcal{L}^{-1}(x)} - 1 \right| dx \tag{32}$$

Comparing [3/1] Padé approximants, the average errors of the Darabi, Eq. 14, and proposed error-minimized [3/1]

approximant, Eq. 30, are 1.257 and 0.4984 %, respectively. Similarly, the error-minimization procedure developed herein reduces the average error associated with [3/2] approximants. The average errors associated with the Cohen, Eq. 11, Jedynek, Eq. 13, and error-minimized [3/2] approximant, Eq. 31, are 2.073, 0.5325, and 0.3538 %, respectively.

Minimized error-corrected approximants

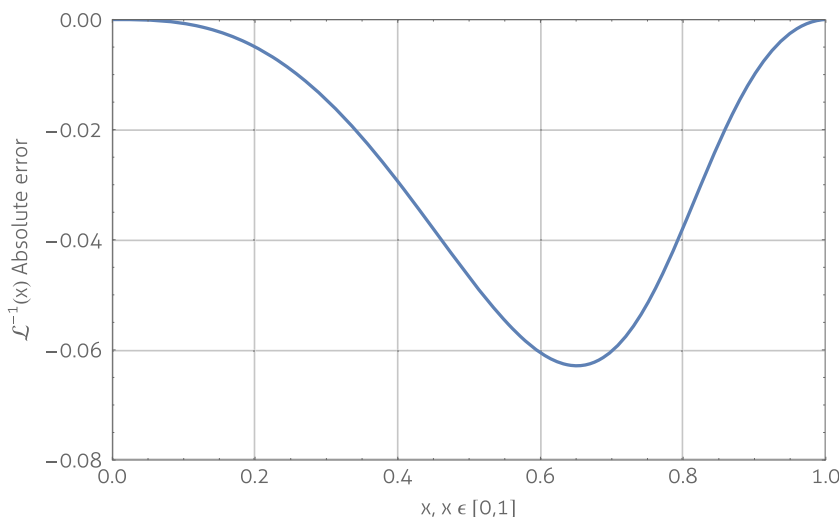
Using the procedure outlined by Beda and Chevalier (2003), and applied to inverse Langevin approximations by Nguessong et al. (2014), it is possible to construct exceedingly accurate and computationally efficient approximations of the inverse Langevin function. Correcting functions act to match the residual error of a particular approximant in an effort to minimize the total error admitted by the new, combined approximant.

Nguessong et al. (2014) presented a 1 step correction to the Cohen approximation, see Eq. 22. The correction function type, Eq. 21, can be applied in its fully general form to further minimize the error committed by the Cohen approximation. Nguessong et al. (2014) placed stringent requirements on the zeros of the correcting function. This level of specificity is not necessary, especially in the context of error minimization of a non-invertible function like the Langevin function.

Furthermore, a similar error correction procedure can be applied to other approximants. Understanding the nature of the absolute error of a particular approximant can inform the selection of error correcting functions. Figure 5 shows the absolute error of the Darabi, Eq. 14, approximant.

The absolute error of the Darabi approximant acts analogously to the residual error of the Cohen approximant following the first step improvement of Nguessong et al.

Fig. 5 Absolute error $(O(x) = \mathcal{L}^{-1}(x) - \mathcal{L}_{\text{approx}}^{-1}(x))$ committed by the Darabi approximant



(2014). Therefore, we propose the use of a polynomial-type correction function of the form

$$\mathcal{L}^{-1}(x) = x \frac{x^2 - 3x + x}{1 - x} + Ax^\alpha (x - \gamma)(x - \delta) \quad (33)$$

to minimize the error admitted by the approximant.

The exact forms of the correcting functions for the Darabi and Cohen approximations can be found using the same optimization techniques implemented in the determination of the error-minimized Padé approximants. Specifically, the minimization objective functions can now be written as

$$\text{minimize}_{A,\alpha,\gamma,\delta} \left\{ \max_{x \in [0,1]} \left| \frac{x \frac{x^2 - 3x + x}{1 - x} + Ax^\alpha (x - \gamma)(x - \delta)}{\mathcal{L}^{-1}(x)} - 1 \right| \right\} \quad (34)$$

and

$$\text{minimize}_{A,\alpha,B,\beta,\gamma,\delta} \left\{ \max_{x \in [0,1]} \left| \frac{x \frac{3-x^2}{1-x^2} + Ax^\alpha + Bx^\beta (x - \gamma)(x - \delta)}{\mathcal{L}^{-1}(x)} - 1 \right| \right\}. \quad (35)$$

Due to the increased complexity of the solution spaces of Eqs. 34 and 35, a combination of optimization techniques was necessary to converge to the global optima. Differential evolution was used to find possible candidate solution vectors within the parameter space using Mathematica. Once possible solution vectors were identified, multiple starting point local minimizations were performed using SQP (Ugray et al. 2007) in MATLAB (MATLAB release 2014a, The MathWorks, Inc., Natick, Massachusetts, USA). The starting points were constructed by randomly perturbing the candidate solution vector determined by the differential evolution algorithm.

By performing the optimizations presented in Eqs. 34 and 35, the parameters of the error-minimized correcting

functions can be determined. The combined forms of the correcting function approximations may be written as

$$\mathcal{L}^{-1}(x) = x \frac{3 - 3x + x^2}{1 - x} + 1.73438x^{3.50505} (x - 0.91867)(x - 1.23956) \quad (36)$$

and

$$\mathcal{L}^{-1}(x) = x \frac{3 - x^2}{1 - x^2} - 0.26965x^{3.13129} - 4.34182x^{8.67624} (x - 1.21532)(x - 1.23027). \quad (37)$$

The error-correcting function containing approximants (36) and (37) are particularly accurate. Figure 6 compares the ability of the minimized relative error approach correcting function approximations to the Bergström approximation and the Ngnessong et al. (2014) Cohen correction.

The proposed optimization methodology cuts the maximum admitted error by the corrected Cohen approximant from $4.654 \times 10^{-2} \%$ (Ngnessong et al. 2014) to $1.457 \times 10^{-2} \%$, representing a 68.70 % improvement with respect to maximum relative error in the domain $x \in [0, 1]$. There is also a reduction in the average error (determined using Eq. 32) admitted by the error-corrected Cohen approximant from $2.061 \times 10^{-2} \%$ (Ngnessong et al. 2014) to $8.079 \times 10^{-3} \%$. Correcting functions have a similar effect on the Darabi approximant, reducing the relative error from 2.639 % to $7.823 \times 10^{-2} \%$. The average error belonging to corrected Darabi approximant is $4.899 \times 10^{-2} \%$.

A more nuanced approximant can be built through a complete optimization of the solution space occupied by both the base approximant and any correcting functions. By optimizing the parameters of the approximant and the correcting function simultaneously the relative error minimization of a

Fig. 6 Percent relative error comparison between error-corrected approximations of the inverse Langevin function

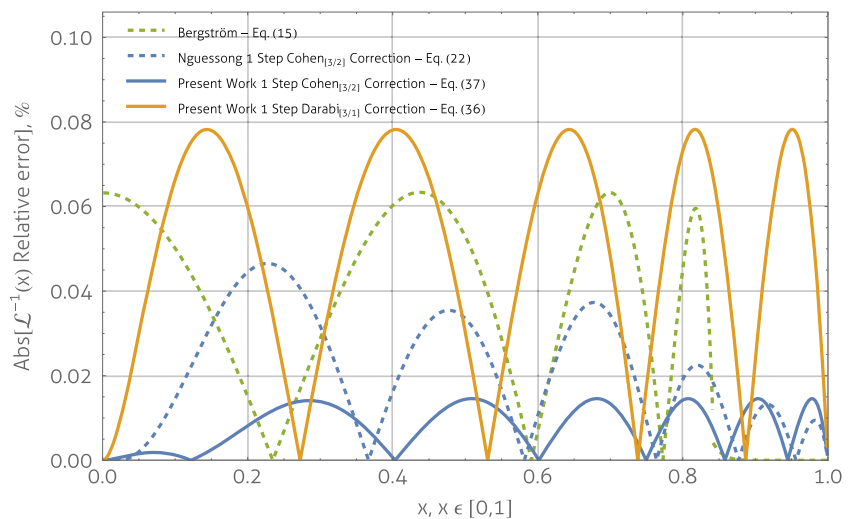
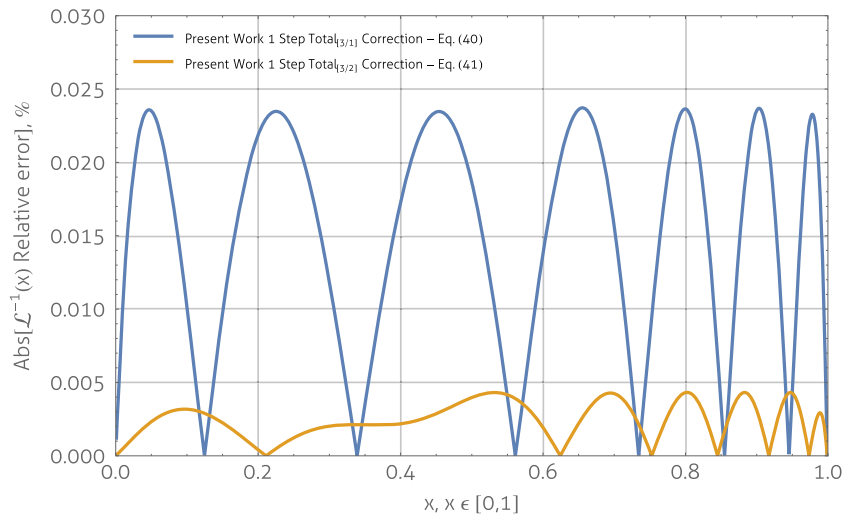


Fig. 7 Percent relative error comparison between completely optimized [3/1] and [3/2] Padé approximants



particular form can be obtained. This procedure was applied in this work to both [3/1] and [3/2] Padé approximants, forming the optimization objectives

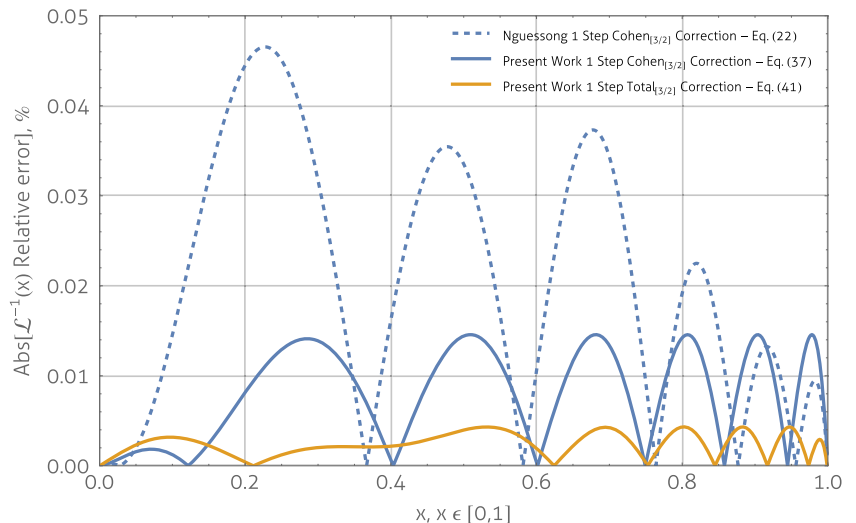
$$\text{minimize}_{\mathbf{a}, A, \alpha, B, \beta, \gamma} \left\{ \max_{x \in [0,1]} \left| \frac{\mathcal{L}_{[3/1]}^{-1}(x, \mathbf{a}) + Ax^\alpha + Bx^\beta(x - \gamma)}{\mathcal{L}^{-1}(x)} - 1 \right| \right\} \tag{38}$$

and

$$\text{minimize}_{\mathbf{b}, A, \alpha, B, \beta, \gamma, \delta} \left\{ \max_{x \in [0,1]} \left| \frac{\mathcal{L}_{[3/2]}^{-1}(x, \mathbf{b}) + Ax^\alpha + Bx^\beta(x - \gamma)(x - \delta)}{\mathcal{L}^{-1}(x)} - 1 \right| \right\}. \tag{39}$$

Combined global (differential evolution) and multiple starting point local (SQP) optimization techniques were

Fig. 8 Percent relative error of corrected [3/2] Padé approximations of the inverse Langevin function



applied to Eqs. 38 and 39, yielding the following error corrected and minimized approximants

$$\mathcal{L}^{-1}(x) = x \frac{-3 + 2.96295x - 0.96292x^2}{x - 1} + 0.28701x^{11.33414} - 1.40114x^{3.42076}(x - 0.78833) \tag{40}$$

and

$$\mathcal{L}^{-1}(x) = x \frac{(3 + (-0.631531 - 0.578498x)x)}{(-1 - 0.789957x)(x - 1)} - 0.44692x^{4.294733} - 11.08867x^{11.60749}(x - 1.004823)(x - 1.022831). \tag{41}$$

Figure 7 illustrates the percent error admitted by the approximants (40) and (41). By allowing the approximant

to dynamically adapt with the correcting function the maximum percent error realized by the [3/1] corrected Padé approximant drops from 7.823×10^{-2} to 2.369×10^{-2} %, with an accompanying average error reduction from 4.899×10^{-2} to 1.505×10^{-2} %. Similarly, the maximum percent error of the [3/2] corrected Padé approximant decreases from 1.457×10^{-2} to 4.315×10^{-3} % and the average error from 8.079×10^{-3} to 2.436×10^{-3} %.

The effectiveness of the combined global and local optimization procedure can be seen in Fig. 8. With increasing freedom in the parameter space, the maximum and average admitted percent error of a particular approximant decreases.

Applications of inverse Langevin approximants

Specified zeroes error-minimized approximants

The development through this point has approached approximating the inverse Langevin function holistically in the domain $x \in [0, 1]$, without any consideration to the real application of the approximant. Network-based models of rubber elasticity built from non-Gaussian descriptions of chain mechanics depend on evaluating the inverse Langevin function. The eight-chain model (Arruda and Boyce 1993) is a three-dimensional, isotropic, hyperelastic constitutive relationship built from a representative volume element that is composed from eight non-Gaussian FJCs with a shared origin at the center of a cube. The chains extend from the center to the corners of the cube. The cube is aligned with the principal stretch directions; therefore, no single chain is aligned with the principal stretches.

Generally, the Cauchy stress tensor can be written as

$$\mathbf{T} = C_r \frac{\sqrt{N}}{\lambda_{\text{chain}}} \mathcal{L}^{-1} \left(\frac{\lambda_{\text{chain}}}{\sqrt{N}} \right) \mathbf{B} - p^* \mathbf{1} \tag{42}$$

where \mathbf{T} is the Cauchy stress tensor, C_r is the rubbery modulus, \sqrt{N} is the locking stretch (λ_{max}), \mathbf{B} is the left Cauchy Green tensor, λ_{chain} is the chain stretch ($\lambda_{\text{chain}} = \sqrt{I_1/3} = \sqrt{\text{tr}(\mathbf{B})/3}$, where I_1 is the first invariant of \mathbf{B}), p^* is the energy indeterminate pressure required by the boundary conditions, and $\mathbf{1}$ is the identity tensor.

It is interesting to note that as $\lambda_{\text{chain}} \rightarrow 1$ (small stretch behavior), $\mathcal{L}^{-1} \left(\lambda_{\text{chain}}/\sqrt{N} \right) \rightarrow \mathcal{L}^{-1} \left(1/\sqrt{N} \right)$. Numerically, this means that as a body begins to deform the inverse Langevin must be evaluated in the neighborhood around $1/\sqrt{N}$. This can be problematic because generally this point, given the particular form of the inverse Langevin approximant, may not have zero relative error. Therefore, at small stretches, there can be substantial, non-continuous error in stress calculations, resulting in stress discontinuities at the onset of deformation. Figure 9 illustrates how the form of the approximation, coupled with the locking stretch of the material, can affect the evolution of error while calculating stresses. The point stress discontinuity at the start of deformation, as λ_{chain} diverges from unity, is clearly shown in Fig. 9.

It is possible to account for this numerical artifact by constructing approximations built to have zero relative error at $x = 1/\sqrt{N}$. Instead of the function requirements specified in Eq. 23 through (25), now, let the approximant be constrained to exactly satisfy the inverse Langevin function at $x = 0, 1/\sqrt{N}$, and 1. Figure 10 demonstrates the capacity of the relative error-minimizing technique to maintain

Fig. 9 Percent relative error of stress in the direction of applied stretch during uniaxial extension of an isotropic, FJC eight-chain material model, $C_r = 1$ MPa and $\sqrt{N} = 2$

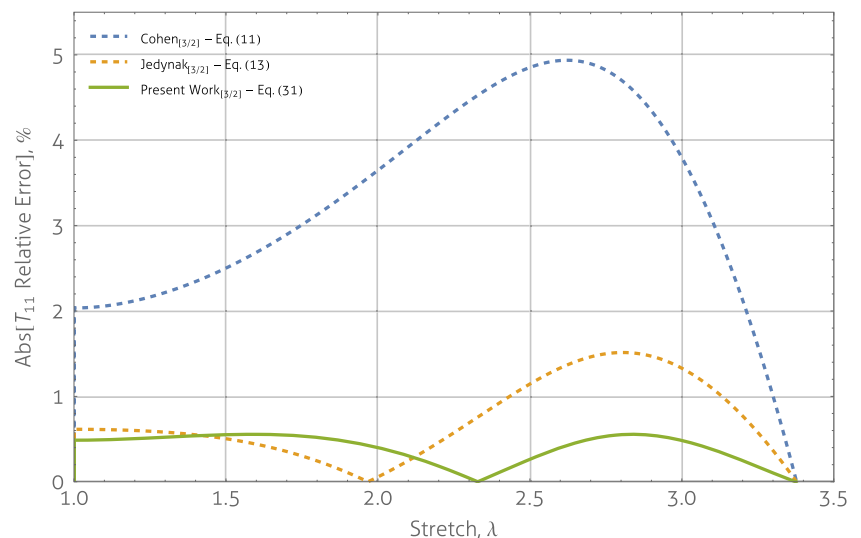
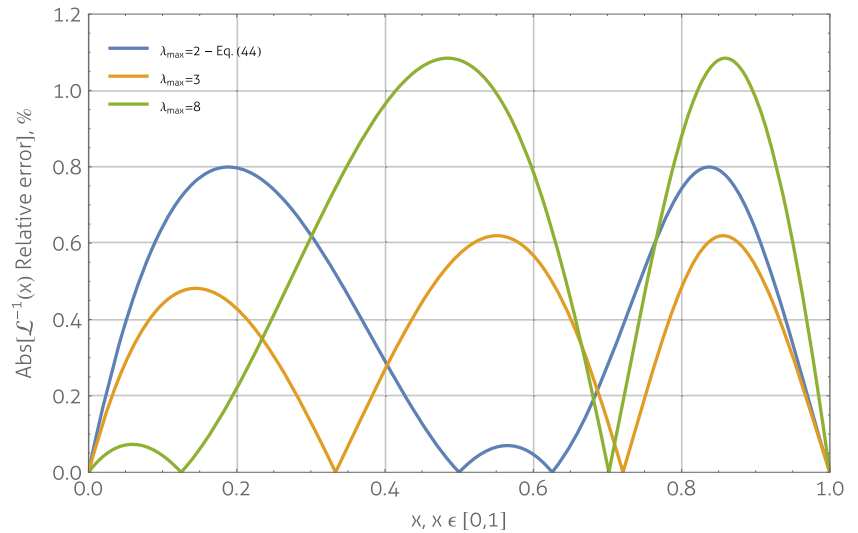


Fig. 10 Percent relative error of [3/2] Padé approximants with specified zeroes determined using differential evolution optimization



domain-wide error control while simultaneously achieving the required small stretch accuracy.

For example, let $\sqrt{N} = \lambda_{\max} = 2$. The error-minimizing optimization objective for determining the specific form of a [3/2] Padé approximant takes the form

$$\text{minimize}_{\mathbf{b}} \left\{ \max_{x \in [0,1]} \left| \frac{1.796756x - 0.898378b_2x + b_1(x^3 - 0.25x) + b_0(x - 0.5)}{(x-1)(b_2x-1)} \mathcal{L}^{-1}(x) - 1 \right| \right\} \quad (43)$$

Solving Eq. 43 the inverse Langevin approximation becomes

$$\mathcal{L}^{-1}(x) = x \frac{2.99997 + x(-3.41905 + 1.18535x)}{(x-1)(0.233723x-1)} \quad (44)$$

The new approximant, shown in Eq. 44, fundamentally changes the relative error associated with calculating the

stress-strain response of materials with constitutive behavior dependent on the inverse Langevin function by removing the point discontinuity at small stretches. In Fig. 11, the relative stress-strain error of [3/2] Padé approximants are shown for uniaxial extension of an isotropic, FJC eight-chain material. Controlling the location of zero error in the domain $x \in [0, 1]$ leads to highly accurate descriptions of stress at the initiation of deformation, with little compromise with respect to error elsewhere in the domain.

Truncated domain error-minimized approximants

The error-minimization framework for determining the specific form of an inverse Langevin approximant proposed in this work can be extended to construct tailored functions optimized for a particular application by appreciating

Fig. 11 Percent relative error comparison of uniaxial stresses evaluated with Cohen, Jedynek, and specified zero error-optimized approximants of the inverse Langevin function

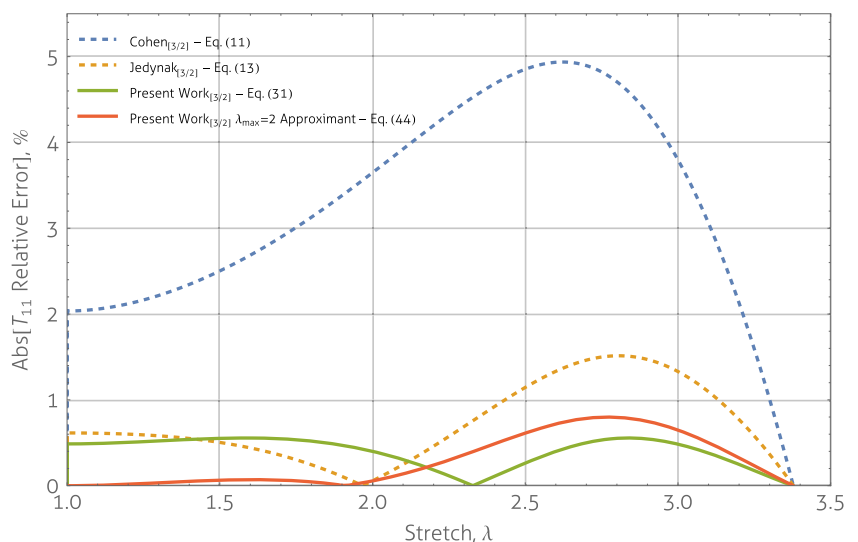
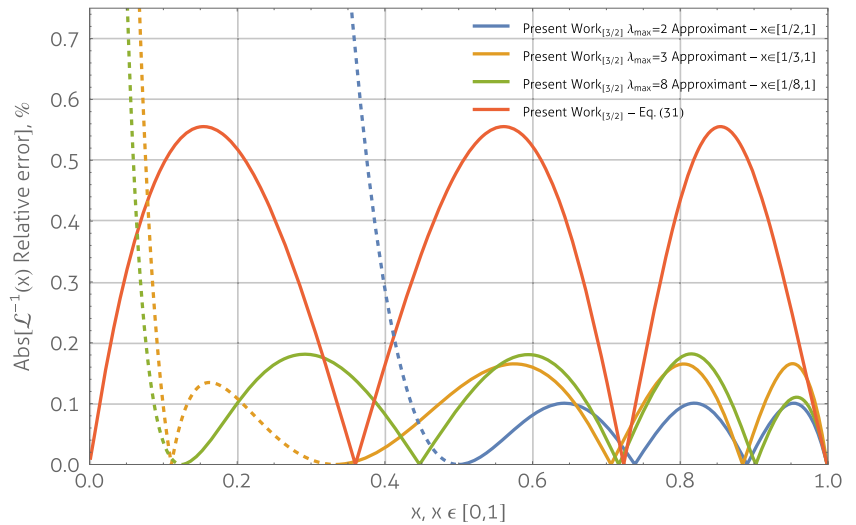


Fig. 12 Percent relative error of approximations with domains $x \in [1/\lambda_{\max}, 1]$. *Solid lines and dashed lines* correspond to percent relative error for approximants in their defined domains $x \in [1/\lambda_{\max}, 1]$ and undefined domains $x \in [0, 1/\lambda_{\max})$, respectively. Approximants were determined using differential evolution



the actual evaluation domain of the inverse Langevin function. Often the argument of a process that requires the computation of the inverse Langevin function occupies a finite region $x \in [a, b]$ with $a > 0$ and $b < 1$. For example, the argument evaluated by the inverse Langevin function in Eq. 42, $\lambda_{\text{chain}}/\sqrt{N}$, is constrained to the domain $\lambda_{\text{chain}}/\sqrt{N} \in [1/\sqrt{N}, 1]$.

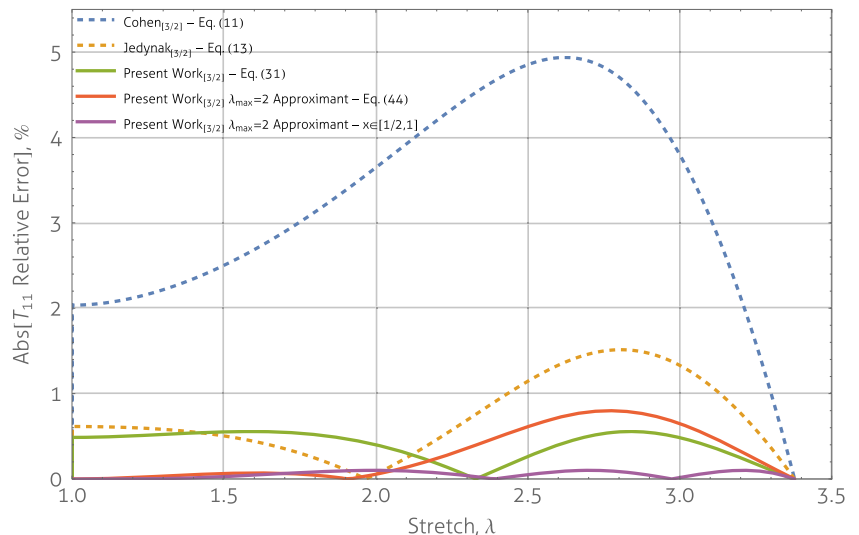
By limiting the optimization domain within the proposed error-minimization framework, it is possible to further refine inverse Langevin approximants without any additional complexity to the form of the function. The general [3/2] approximant can be reformulated by imposing constraints on the behavior at the boundaries of the domain at $x = 1/\sqrt{N}$ and $x = 1$ similar to the conditions for the unconstrained domain approximant (Eq. 23 through (25)). Maintaining the constraint presented in Eq. 25 and requiring the value of the approximant and its derivative to be

exactly satisfied at $x = 1/\sqrt{N}$, the [3/2] Padé approximant optimized for the domain $x \in [1/\sqrt{N}, 1]$ can be written as

$$\mathcal{L}_{[3/2]}^{-1}(x, \mathbf{b}, N) = \frac{1}{N^{3/2}(x-1)(b_2x-1)} \left\{ -\sqrt{N}(b_2 + N(x-1)) + b_2(N - 2\sqrt{N})x \mathcal{L}^{-1}(1/\sqrt{N}) + (\sqrt{Nx} - 1) \left((\sqrt{Nx} - 1)(2b_1 + b_0\sqrt{N} + b_1\sqrt{Nx}) + (b_2 - (1 + b_2)\sqrt{N} + N) \frac{\partial \mathcal{L}^{-1}(x)}{\partial x} \Big|_{x=1/\sqrt{N}} \right) \right\} \quad (45)$$

where $\mathcal{L}^{-1}(1/\sqrt{N})$ and $\frac{\partial \mathcal{L}^{-1}}{\partial x} \Big|_{x=1/\sqrt{N}}$ are the exact values of the inverse Langevin function and its derivative at $x = 1/\sqrt{N}$, respectively. This form holds $\forall N \in (1, \infty)$, with the general form of the [3/2] Padé approximant for the inverse Langevin function, Eq. 45, reducing in the

Fig. 13 Percent relative error comparison of uniaxial stresses evaluated with various approximants of the inverse Langevin function



limit as $N \rightarrow \infty$ to whole domain, $x \in [0, 1]$, approximant, Eq. 27.

Using the general form for the [3/2] Padé approximant, Eq. 45, it is possible to construct a new optimization objective using the proposed error-minimization method presented in this work for the domain $x \in [1/\sqrt{N}, 1] = [1/\lambda_{\max}, 1]$ as

$$\text{minimize}_{\mathbf{b}} \left\{ \max_{x \in [1/\sqrt{N}, 1]} \left| \frac{\mathcal{L}_{[3/2]}^{-1}(x, \mathbf{b}, N)}{\mathcal{L}^{-1}(x)} - 1 \right| \right\}. \quad (46)$$

Note that the optimization problem presented in Eq. 46 is a function the number of chain links, N . Equation 46 can be solved using any of the optimization techniques discussed herein. Figure 12 shows the relative error of [3/2]

approximants with various locking stretches compared with the whole domain approximant, Eq. 31.

Intelligently selecting and optimizing over a discrete domain reduces the maximum and average relative errors of [3/2] Padé approximants. The increase in accuracy within the reduced domain is achieved by pushing the error committed by the approximant into the domain where the function is undefined (this phenomenon can be observed in Fig. 12 as the solid lines transition to dashed lines and the error functions become unbounded).

Truncated domain approximants built using the proposed error-minimization technique—solving the optimization problem presented in Eq. 46 for specific values of N —are capable of producing increasingly accurate approximations of the inverse Langevin function, given the application does not require determining the inverse Langevin of an argument outside the domain used to construct the

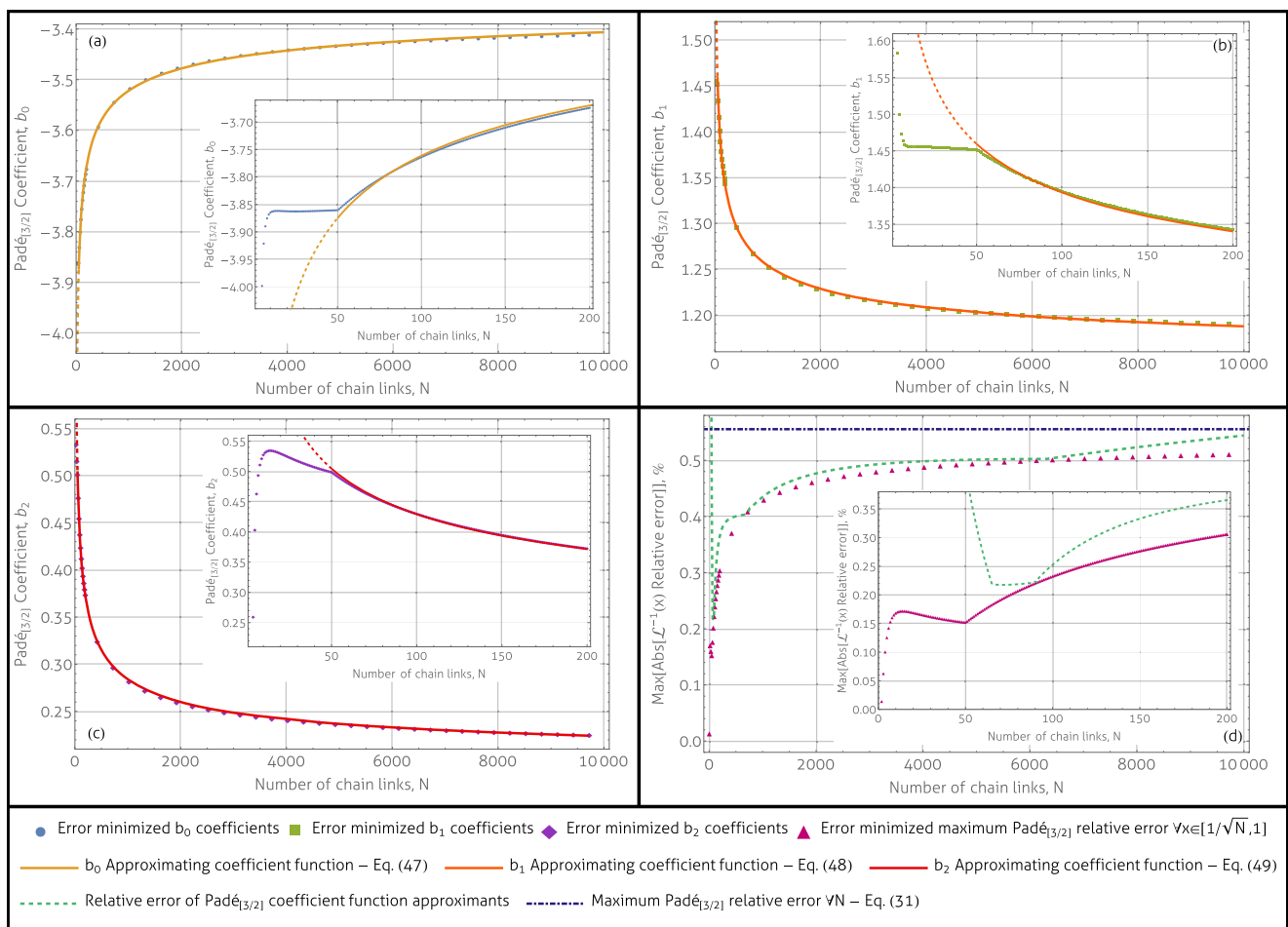


Fig. 14 a–c Error-minimized [3/2] Padé approximant coefficient b_0 , b_1 , b_2 (points) as a function of the number of chain links, N , respectively. Equations (47) through (49) are plotted *solid* for $N \geq 50$ and *dashed* for $N < 50$ in (a), (b), and (c), respectively. The error-minimized coefficients, and divergence of Eq. 47 through (49) from their respective error-minimized coefficients, at small locking

stretches are also presented in the subplots of (a), (b), and (c), respectively. **d** Maximum relative error of discrete domain [3/2] Padé approximants constructed from error-minimized coefficients (points) and approximant coefficients (*dashed line*)—approximant coefficients determined by Eq. 47 through (49)—compared to the maximum relative error of Eq. 31 (*dot dashed line*)

particular form of the approximant. Figure 13 depicts the relative percent error of the stress-strain relationships—in uniaxial extension—of [3/2] Padé approximants (Cohen, Eq. 11; Jedynek, Eq. 13; error minimized for the domain $x \in [0, 1]$, Eq. 31; error minimized for the domain $x \in [0, 1]$ fixed with zero relative error at $x = 1/\lambda_{\max}$, Eq. 44; error minimized for the domain $x \in [1/\lambda_{\max}, 1]$) for $\lambda_{\max} = 2$.

The optimization problem presented in Eq. 46 can be used to determine the relationship between coefficients of [3/2] Padé approximants, $\mathbf{b} = \{b_0, b_1, b_2\}$, and the number of chain links, N . We found that for large locking stretches, the error-minimized Padé coefficients were well behaved and capable of being defined through a power law. The relationships between the coefficients and the number of chain links were determined using a nonlinear least squares regression for $N > 50$. Explicitly, the large locking stretch coefficient relationships were calculated as

$$b_0(N) = -3.300 - \frac{1.999}{N^{0.3184}}, \quad N \geq 50, \quad (47)$$

$$b_1(N) = 1.128 + \frac{1.172}{N^{0.3224}}, \quad N \geq 50, \quad (48)$$

and

$$b_2(N) = 0.1810 + \frac{1.442}{N^{0.3820}}, \quad N \geq 50. \quad (49)$$

Equations 47 through (49) have adjusted R^2 , coefficient of determination, values of 1.0000, 1.0000, and 0.99999, respectively.

An exhaustive description of the relationships between the coefficients of error-minimized, discrete domain [3/2] Padé approximants, $\mathbf{b} = \{b_0, b_1, b_2\}$, and the number of chain links, N , are presented in Fig. 14a–d. The Padé coefficients were found by solving Eq. 46 for a particular N using differential evolution; the maximum associated relative error was also determined. As the locking stretch increases the Padé coefficients tend toward their corresponding values in Eq. 31; the maximum relative error, predictably, has similar behavior.

It is clear for small values of N , $N < 50$, there is significant deviation from the optimal Padé coefficients while using the relationships presented in Eq. 47 through (49), leading to increasingly lower accuracy approximants of the inverse Langevin with decreasing N . This trend is exactly opposite to the maximum error behavior using the optimal coefficients (see the divergence of the dashed line from the data points in Fig. 14d for small N). It is also important to note that though the maximum relative error of the approximant built using Padé coefficient functions (Eq. 47 through (49)) is greater than that of the optimal Padé coefficients, due to the form of the inverse Langevin approximant, Eq. 45, the behavior at the boundaries of the domain are automatically satisfied.

For applications with large locking stretches, $N \geq 50$, it is possible to combine the approximant Padé coefficient functions, Eq. 47 through (49), with the general form of the [3/2] Padé approximant for the inverse Langevin function, Eq. 45, to simplify the optimization problem shown in Eq. 46. The coefficient functions reduce the complexity of finding a particular inverse Langevin approximant from an optimization problem to simply determining the exact value of the inverse Langevin and its derivation at a single point.

Conclusions

An error-minimization approach for determining inverse approximants of non-invertible functions has been developed using a combined gradient-based and direct search optimization procedure. The technique has been shown to reduce the relative and average errors admitted by approximants by distributing the committed error over the entire function domain. Padé approximants of the inverse Langevin function were reformulated in this framework to determine their error-minimized form. This method produces approximants with increased accuracy, with relatively no computational tradeoff. The method was extended to more complex approximant forms, including power and polynomial error correcting functions. All the approximants produced by this technique are readily evaluated, differentiated, and integrated, and their implementation in existing computational methods—like finite element methods—is straightforward.

Often the application of the inverse Langevin approximant can be used to inform its construction. Using network-based models of rubber elasticity assembled with non-Gaussian chain descriptions (specifically, the eight-chain model developed by Arruda and Boyce (1993)) as a prototypical example, the error-minimizing framework was also used to build optimized approximants with specified mid-domain behavior and reduced domains. In the context of the eight-chain model, approximations of the inverse Langevin function can admit non-continuous error at small stretches. This phenomenon leads to stress discontinuities at the start of deformation. Stress discontinuities can be removed by explicitly requiring the form of the inverse Langevin approximant to have zero error at small stretches. Additionally, in certain applications, the accuracy of a particular approximant can be improved by understanding the function’s evaluation domain. We have shown that for a domain $x \in [a, 1]$, for $0 \leq a \leq 1$, a common evaluation domain of constitutive models of rubber elasticity, it is possible to construct a general form of the [3/2] Padé approximant that can be used in the proposed error-minimizing framework to determine the particular, error-minimized, truncated domain inverse Langevin approximant. The truncated

domain approach simultaneously reduces the maximum and average relative error admitted by the approximant, compared to the equivalent whole domain approximant, while eliminating stress discontinuities at the onset of deformation.

References

- Arruda EM, Boyce MC (1993) A three-dimensional constitutive model for the large stretch behavior of rubber elastic materials. *J Mech Phys Solids* 41(2):389–412
- Beda T, Chevalier Y (2003) Non-linear approximation method by an approach in stages. *Comput Mech* 32(3):177–184
- Bergström JS (1999) Large strain time-dependent behavior of elastomeric materials. PhD thesis, Massachusetts Institute of Technology
- Bischoff JE, Arruda EM, Grosh K (2002a) Finite element simulations of orthotropic hyperelasticity. *Comput Mech* 38(10):983–998
- Bischoff JE, Arruda EM, Grosh K (2002b) A microstructurally based orthotropic hyperelastic constitutive law. *J Appl Mech* 69(5):570–579
- Boggs PT, Tolle JW (1995) Sequential quadratic programming. *Acta Numerica* 4:1–51
- Boyce MC, Arruda EM (2000) Constitutive models of rubber elasticity: a review. *Rubber Chem Technol* 73(3):504–523
- Cohen A (1991) A Padé approximant to the inverse Langevin function. *Rheol Acta* 30(3):270–273
- Darabi E, Itskov M (2015) A simple and accurate approximation of the inverse Langevin function. *Rheol Acta* 54(5):455–459
- Dargazany R, Hörmes K, Itskov M (2013) A simple algorithm for the fast calculation of higher order derivatives of the inverse function. *Appl Math Comput* 221:833–838
- Flory PJ, Erman B (1982) Theory of elasticity of polymer networks. 3. *Macromolecules* 15(3):800–806
- Holub A (2003) Method of generalized moment representations in the theory of rational approximation (a survey). *Ukr Math J* 55(3):377–433
- Itskov M, Ehret AE, Dargazany R (2009) A full-network rubber elasticity model based on analytical integration. *Mathematics and Mechanics of Solids*
- Itskov M, Dargazany R, Hörmes K (2012) Taylor expansion of the inverse function with application to the Langevin function. *Mathematics and Mechanics of Solids*. p 1081286511429886
- Jedynak R (2015) Approximation of the inverse Langevin function revisited. *Rheol Acta* 54(1):29–39
- Kang I, Panneerselvam D, Panoskaltis VP, Eppell SJ, Marchant RE, Doerschuk CM (2008) Changes in the hyperelastic properties of endothelial cells induced by tumor necrosis factor- α . *Biophys J* 94(8):3273–3285
- Kröger M (2015) Simple, admissible, and accurate approximants of the inverse Langevin and Brillouin functions, relevant for strong polymer deformations and flows. *Journal of Non-Newtonian Fluid Mechanics*
- Kuhl E, Garikipati K, Arruda EM, Grosh K (2005) Remodeling of biological tissue: mechanically induced reorientation of a transversely isotropic chain network. *J Mech Phys Solids* 53(7):1552–1573
- Kuhn W, Grin F (1942) Beziehungen zwischen elastischen konstanten und dehnungs-doppelbrechung hochelastischer stoffe. *Kolloid Z* 101(3):248–271
- Ma J, Arruda EM (2013) A micromechanical viscoelastic constitutive model for native and engineered anterior cruciate ligaments. In: *Computer models in biomechanics*. Springer, Berlin, pp 351–363
- Ma J, Narayanan H, Garikipati K, Grosh K, Arruda E (2010) Experimental and computational investigation of viscoelasticity of native and engineered ligament and tendon. In: *IUTAM symposium on cellular, molecular and tissue mechanics*. Springer, Berlin, pp 3–17
- Nguessong AN, Beda T, Peyraud F (2014) A new based error approach to approximate the inverse Langevin function. *Rheol Acta* 53(8):585–591
- Palmer JS, Boyce MC (2008) Constitutive modeling of the stress-strain behavior of f-actin filament networks. *Acta Biomater* 4(3):597–612
- Puso MA (1994) Mechanistic constitutive models for rubber elasticity and viscoelasticity. PhD thesis, University of California, Davis
- Storn R, Price K (1997) Differential evolution—a simple and efficient heuristic for global optimization over continuous spaces. *J Glob Optim* 11(4):341–359
- Treloar LRG (1975) *The physics of rubber elasticity*. Oxford University Press, London
- Ugray Z, Lasdon L, Plummer J, Glover F, Kelly J, Martí R (2007) Scatter search and local nlp solvers: a multistart framework for global optimization. *INFORMS J Comput* 19(3):328–340
- Wang MC, Guth E (1952) Statistical theory of networks of non-gaussian flexible chains. *J Chem Phys* 20(7):1144–1157
- Warner Jr HR (1972) Kinetic theory and rheology of dilute suspensions of finitely extendible dumbbells. *Ind Eng Chem Fundam* 11(3):379–387
- Wu P, Van der Giessen E (1993) On improved network models for rubber elasticity and their applications to orientation hardening in glassy polymers. *J Mech Phys Solids* 41(3):427–456